Afferent–Target Cell Interactions in the Cerebellum: Negative Effect of Granule Cells on Purkinje Cell Development in Lurcher Mice

Martin L. Doughty,[1] **Ann Lohof,**[1,2] **Fekrije Selimi,**[1] **Nicole Delhaye-Bouchaud,**[1] **and Jean Mariani**[1]

[1]*Laboratoire de Neurobiologie du Développement, Institut des Neurosciences (Unite Mixte de Recherche 7624), Université Pierre et Marie Curie, 75005 Paris, France, and* [2]*Laboratoire de Neurobiologie, Ecole Normale Supérieure, 75005 Paris, France*

Lurcher (*Lc*) is a gain-of-function mutation in the δ2 glutamate receptor gene that results in a large, constitutive inward current in the cerebellar Purkinje cells of +/*Lc* mice. +/*Lc* Purkinje cells fail to differentiate fully and die during postnatal development. In normal mice, interactions with granule cells promote Purkinje cell dendritic differentiation. Partial destruction of the granule cell population in young +/*Lc* mice by x irradiation resulted in a significant increase in Purkinje cell dendritic growth and improved cytoplasmic structure but did not prevent Purkinje cell death. These results indicate two components to Purkinje cell abnormalities in +/*Lc* mice: a retardation/blockade of dendritic development that is mediated by interactions with granule cells and the death of the cell. Thus, the normal trophic effects of granule cell interaction on Purkinje cell development are absent in the +/*Lc* cerebellum, suggesting that granule cells are powerful regulators of Purkinje cell differentiation.

Key words: Lurcher; Purkinje cell; dendrites; granule cell; parallel fiber; synapse; delta 2 glutamate receptor

The formation of synapses requires the coordinated growth and differentiation of afferents and target cells. Coordination is achieved through a combination of intrinsic genetic programs (Hatten et al., 1997) and extrinsic regulatory factors supplied by the cellular environment and appropriate synaptic partners (Tessier-Lavigne and Goodman, 1996). Although much interest has focused on the regulation of afferent axon growth by the target cell (e.g., Porter et al., 1995; Davis et al., 1997), afferent–target cell interactions appear to be reciprocal in the development of a number of synaptic connections.

In the cerebellum, granule cells interact reciprocally with both their presynaptic afferent mossy fibers and their postsynaptic target Purkinje cells. For example, tissue culture experiments indicate that mossy fiber innervation, which arises from the specific arrest of afferent axon growth by the target cell (Baird et al., 1992), in turn induces the alteration in expression of NMDA receptor subunits in the developing granule cell (Ozaki et al., 1997). Furthermore, these processes are dependent on NMDA receptor activation (Baird et al., 1996; Ozaki et al., 1997), implicating the involvement of synaptic activity. Analyses of Purkinje cell development in animal models with afferent lesions (Sotelo, 1975; Altman and Bayer, 1997) and in culture (Baptista et al., 1994) indicate that granule cells regulate Purkinje cell differentiation through a complex balance of neurotrophin- and activity-dependent signaling (Morrison and Mason, 1998). Correspond-

ingly, evidence from several genetic mouse models has demonstrated the involvement of the Purkinje cell in the regulation of granule cell proliferation (Yoon, 1976; Feddersen et al., 1992), differentiation, and survival (Sotelo and Changeux, 1974; Caddy and Biscoe, 1979; Herrup and Sunter, 1986).

The heterozygous Lurcher (+/*Lc*) mutant mouse provides a convenient model to study cerebellar afferent–target cell interactions *in vivo*. The Purkinje cells of +/*Lc* mice fail to differentiate fully and die during postnatal development (Caddy and Biscoe, 1979) owing to a gain-of-function mutation of the δ2 glutamate receptor subunit (GluRδ2) gene that results in a large, constitutive inward current in the cell (Zuo et al., 1997). The onset of morphological abnormalities in +/*Lc* Purkinje cells coincides with the innervation of the cell by granule cell parallel fibers (Dumesnil-Bousez and Sotelo, 1992). In normal mice, GluRδ2 becomes localized to the postsynaptic dendritic spines of Purkinje cells during parallel fiber synaptogenesis (Takayama et al., 1996; Landsend et al., 1997), where it is speculated to be involved in the stabilization of the synapse (Kurihara et al., 1997). The correlation between the initiation of parallel fiber synaptogenesis, the onset of morphological abnormalities in +/*Lc* mice, and the normal localization of the GluRδ2 protein suggest that interactions with the afferent granule cell may influence +/*Lc* Purkinje cell development.

We have investigated the role of granule cell interaction in the development and death of Purkinje cells in +/*Lc* mice by reducing the afferent population *in vivo* with localized x irradiation. The decrease in granule cell numbers resulted in a significant increase in Purkinje cell dendritic growth and improved cytoplasmic structure but did not prevent the death of the cell. These results demonstrate that the normal trophic effects of granule cell interaction on Purkinje cell development are absent in the +/*Lc* cerebellum. The negative effects of granule cell interaction in +/*Lc* mice suggest that the parallel fiber is a powerful regulator of Purkinje cell dendritic growth. The results also indicate two separate components to the Purkinje cell abnormalities seen in

+/*Lc* mice: a retardation/blockade of development, and cell death.

MATERIALS AND METHODS

Animals. Lurcher (+/*Lc*) mice were generated by crosses using a B6CBA strain of inbred mice that carry the mutation. For all matings, wild-type (+/+) B6CBA females were crossed with heterozygous Lurcher (+/*Lc*) males. The animals were provided with food and water *ad libitum* and housed under standard conditions (12 hr light/dark cycle, 22°C). All animal procedures were performed under the guidelines established by "le comité consultatif national d'éthique pour les sciences de la vie et de la santé".

X-irradiation schedule. All the pups (6–10) in a litter from a +/+ × +/*Lc* mating were exposed to x irradiation localized to the hindbrain. The pups were exposed to 500 rads of x irradiation on postnatal day 5 (P5) using the procedure described in Crepel et al. (1976). In response to the x irradiation dose, the mice developed an ataxia in the second postnatal week. Nevertheless, under careful observation, P15 and older x-irradiated +/*Lc* mice exhibit a sprawling gait and swaying motion that is distinct from the ataxia induced by the x rays in +/+ littermates. In this manner, x-irradiated +/*Lc* and +/+ littermates were distinguished; their genotypes were later histologically confirmed.

Light microscopy. All animals from a litter (P15–P30) were deeply anesthetized with an intraperitoneal injection of chloral hydrate and perfused intracardially with 0.9% NaCl followed by 95% ethanol. The brain was dissected out and post-fixed at 4°C overnight in 75% ethanol, 25% acetic acid, dehydrated and embedded in paraffin. Midsagittal cerebellar sections (10-μm-thick) were cut, deparaffinized, and incubated with mouse monoclonal anti-Calbindin (anti-CaBP) antibodies (Sigma, St. Louis, MO; 1:300 dilution) overnight at 4°C. The CaBP-immuno-labeled sections were processed using Vectashield ABC kit (Vector Laboratories, Burlingame, CA) according to the manufacturer's instructions and visualized with DAB (Sigma). Some CaBP-immunolabeled sections were stained with cresyl violet–thionin as were adjacent, non-immunolabeled cerebellar sections. Controls were performed with either the primary or secondary antibody incubation deleted.

Cell counts and morphometric analysis. The number of granule cells per section was estimated from midsagittal cerebellar sections stained with cresyl violet–thionin. The number of granule cells per section was estimated from the total area of the internal granule cell layer (IGL) multiplied by the density of granule cells within the IGL. The area of the IGL was measured from a captured image of the cerebellar section. The image of the cerebellum was captured on a video graphics card using NIH Image software and a CCD video camera attached to a Nikon microscope at 20× magnification. The IGL of the captured image was outlined freehand, and the area enclosed was measured using NIH Image software. The density of granule cells in the IGL was estimated from the number of granule cells enclosed in a 3600 μm^2 area defined by an ocular graticule at 1000× magnification. Granule cell counts were taken from the posterior, middle, and anterior cerebellum and used to calculate an average cell density. The area of the Purkinje cell dendritic tree was estimated from images captured from midsagittal cerebellar sections processed for anti-CaBP immunocytochemistry. Purkinje cells were first selected randomly at low magnification (40×) from lobules VI, V, IV and III, and the CaBP-immunostained Purkinje cell image was then captured on a video graphics card using NIH Image software and a CCD video camera attached to a Nikon microscope at 200× magnification. The dendritic tree of the captured Purkinje cell image was outlined freehand, and the area enclosed was measured using NIH Image software. A Purkinje cell was excluded from the analysis if it was very faintly stained, if it lacked a visible dendritic tree, or if its dendritic tree could not be reliably distinguished from those of adjacent cells. The height of CaBP-immunostained Purkinje cells from the base of the cell body to the distal tip of the dendrites was measured from the same cerebellar sections using a camera lucida at 250× magnification. For both measurements, 10–20 Purkinje cells were analyzed per animal, and the data were used to calculate an average. The number of Purkinje cells per section was estimated from midsagittal cerebellar sections processed for anti-CaBP immunocytochemistry and cresyl-violet-thionin staining. The total number of CaBP-immunostained cell bodies in the Purkinje cell layer (PCL) and molecular layer (ML) of the section was counted at 200× magnification using Nomarski optics.

Electron microscopy. The mice (P20) were deeply anesthetized with an intraperitoneal injection of chloral hydrate and perfused intracardially with 1% paraformaldehyde, 1% glutaraldehyde in 0.1 M phosphate buffer (PB), pH 7.4, followed by 6% glutaraldehyde in 0.1 M PB. The brain was dissected out and post-fixed at 4°C overnight in 6% glutaraldehyde in 0.1 M PB. The cerebellum was sectioned sagittally at ~1 mm thickness, and the slices were post-fixed in 2% osmium tetroxide (OsO$_4$) in 0.1 M PB, dehydrated, and embedded in Epon 812. Thin sections (50–70 nm) were cut from the cerebellar cortex using a Reichert ultramicrotome, collected on copper mesh grids, and stained with a saturated solution of uranyl acetate in methanol, followed by a 2.6% solution of lead citrate. The sections were examined using a Philips transmission electron microscope.

Electrophysiology. Cerebellar slices were prepared from P15–P20 mice using standard procedures (Llano et al., 1991). Animals were decapitated, and the cerebellum was rapidly removed and dissected in ice-cold buffer containing (in mM) 125 NaCl, 2.5 KCl, 1.25 NaH$_2$PO$_4$, 26 NaHCO$_3$, 2 CaCl$_2$, 1 MgCl$_2$, 25 glucose, continuously bubbled with 95% O$_2$ and 5% CO$_2$. Sagittal slices were cut at 250 μm and allowed to recover in the same buffer at 35°C for 1 hr before recording began. The slice recording chamber was continuously superfused with the buffer described above at room temperature. The *N*-methyl-D-glucamine (NMDG)-substituted buffer replaced the NaCl with 136 mM NMDG. The superfusion buffers contained 10 μM bicuculline methochloride to block inhibitory synaptic currents. Whole-cell patch-clamp recordings were made from Purkinje cells using an Axopatch 200 amplifier (Axon Instruments, Foster City, CA); data were acquired with PClamp6 (Axon Instruments) and analyzed with IgorPro (WaveMetrics, Lake Oswego, OR). Patch pipettes were filled with a solution containing (in mM) 6 KCl, 140 K D-gluconate, 10 HEPES, 1 EGTA, 0.1 CaCl$_2$, 5 MgCl$_2$, 4 Na$_2$ATP, and 0.4 NaGTP, pH 7.3, 290–300 mOsm. Purkinje cells were voltage-clamped at −70 mV while recording the leak currents, and the recording mode changed to current-clamp from time to time to monitor the resting potential. The morphology of the cerebellar slices not used for recording was examined to confirm the +/*Lc* or +/+ genotype of the mouse. Briefly, the slices were fixed in a solution of 4% paraformaldehyde in 0.1 M PB overnight and transferred to a cryoprotectant solution of 10% polyvinyl-pyrrolidone, 6% sucrose for 3 d (all at 4°C), sectioned (14-μm-thick) on a cryostat, and stained with cresyl violet–thionin.

RESULTS

A single dose of x irradiation results in large-scale granule cell loss

We used x irradiation to destroy the dividing granule cell precursors in the cerebellum of young +/*Lc* and +/+ mice. Ionizing radiation induces DNA fragmentation and apoptosis in dividing cells by the production of free radicals (Wood and Youle, 1995). We exposed pups to a single dose of 500 rads of x irradiation on P5 and examined the cerebella 10–25 d later. Figure 1 shows the effects of the x rays on the cerebella of +/*Lc* and +/+ mice at P15. The extent of granule cell destruction caused by the x rays is best observed in the +/+ mice because the +/*Lc* mutation results in prolonged granule cell death following the loss of the target Purkinje cell (Caddy and Biscoe, 1979). The cerebella of x-irradiated +/+ mice are greatly reduced in size, and the IGL is thinner and less cell-dense, reflecting large-scale granule cell loss. Similarly, the cerebella of x-irradiated +/*Lc* mice are smaller than in the nonirradiated mutant, and the IGL is thinner and less cell-dense at P15. At P20, the IGL of x-irradiated +/*Lc* mice remains smaller than that of nonirradiated mutants, but the granule cell densities are similar. By P30, granule cell loss from the effects of the *Lc* mutation results in a similarly reduced IGL in the x-irradiated and nonirradiated mutant. We estimated the number of granule cells per midsagittal section in P15, P20, and P30 x-irradiated and nonirradiated +/+ and +/*Lc* mice (Table 1). The results indicate a consistent 75% reduction in the number of granule cells in x-irradiated +/+ mice. The data from the non-irradiated +/*Lc* mouse indicate that only 50% of the granule cell population remained at P15 as a result of target-related granule cell loss. Exposure to x rays reduces the number of granule cells in the P15 +/*Lc* mice by more than half, to only 23% of the normal +/+ value. The number of granule cells per section in the
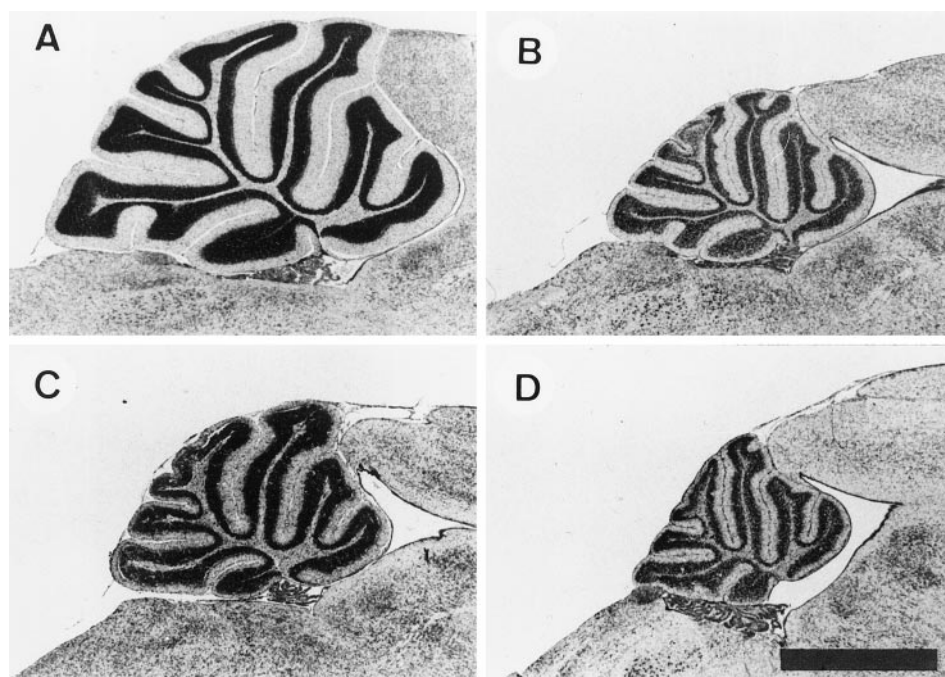
Figure 1. The effects of localized x irradiation of the hindbrain. Midsagittal cerebellar sections of P15 mice stained with cresyl violet–thionin. *A*, Nonirradiated wild-type (+/+) mouse. *B*, X-irradiated +/+ mouse. *C*, Nonirradiated Lurcher (+/*Lc*) mouse. *D*, X-irradiated +/*Lc* mouse. The x-irradiated mice were exposed to 500 rads of x rays on P5. The x-ray dose destroys 70% of the granule cell population, a loss that is augmented by target-related cell death in the +/*Lc* mouse. Scale bar, 1 mm.

Table 1. Estimated number of granule cells per midsagittal section and percentage value of the wild-type control

	+/+	+/+ irrad.	+/*Lc*	+/*Lc* irrad.
P15	58688 ± 1959	16016 ± 1636*	29563 ± 1729	13417 ± 998*
	100%	27%	50%	23%
P20	68739 ± 2057	16315 ± 1690*	20496 ± 1034	13410 ± 372*
	100%	24%	30%	20%
P30	71345 ± 3270	17880**	10256 ± 803	8190 ± 808
	100%	25%	14%	11%

+/+, Wild-type; +/*Lc*, Lurcher; irrad, x-irradiated on P5.

Mean ± SEM, *n* = 3 in all cases except **n = 1.

*Different from nonirradiated control (Mann–Whitney *U* test, *p* < 0.05).

x-irradiated +/*Lc* mice (20%) remains below that of the nonirradiated (30%) mutant at P20, but the difference is less than at P15. In older animals, the differences in granule cell number between the x-irradiated and nonirradiated +/*Lc* mice diminish as target-related granule cell loss continues. At P30, the number of granule cells in the x-irradiated and nonirradiated +/*Lc* mice are 14 and 11%, respectively, of the +/+ value. The cell counts demonstrate that a single dose of 500 rads of x irradiation on P5 destroys 70% of the granule cell population, a loss that is augmented by target-related cell death in the +/*Lc* mouse. Hence, in the case of +/*Lc* mice, x irradiation results in the premature loss of granule cells.

Increased Purkinje cell dendritic development in +/*Lc* mice after the partial destruction of granule cells by x rays

Before cell death, +/*Lc* Purkinje cells exhibit characteristic dendritic abnormalities: the stems of the dendrites are thicker but the spread of the dendritic tree is reduced and less branched when compared with +/+ Purkinje cells (Caddy and Biscoe, 1979; Dumesnil-Bousez and Sotelo, 1992). We examined the effects of granule cell destruction on the dendritic development of +/*Lc* Purkinje cells. To aid the identification of Purkinje cells, we immunolabeled sections with a monoclonal antibody to Calbindin (CaBP). In the cerebellar cortex, CaBP immunoreactivity is specific to Purkinje cells and is present throughout the cell from early in embryonic development (Legrand et al., 1983). At P15, the thickened dendrites of Purkinje cells in sections from nonirradiated +/*Lc* mice are poorly branched and fail to reach the pial surface as in the +/+. In contrast, the dendritic trees of Purkinje cells in sections from x-irradiated +/*Lc* mice are more branched and extend to the pial surface (although they remain underdeveloped when compared with the +/+). This pattern of increased dendritic development in the x-irradiated compared with nonirradiated +/*Lc* mice is more evident in sections from older animals (Fig. 2). The dendritic trees of some, but not all, of the Purkinje cells remaining in sections from P20–P30 x-irradiated +/*Lc* mice have elaborate, highly branched dendritic trees that extend to the pial surface and spread laterally across the molecular layer; the dendritic trees of all of the remaining Purkinje cells in sections from P20–P30 nonirradiated +/*Lc* mice fail to reach the pial surface (often barely reaching the mid ML), and the thickened dendritic shafts contain few lateral branches. In contrast to the increased growth observed in +/*Lc* mice, the effects of the reduction of the granule cell population by x rays in +/+ mice
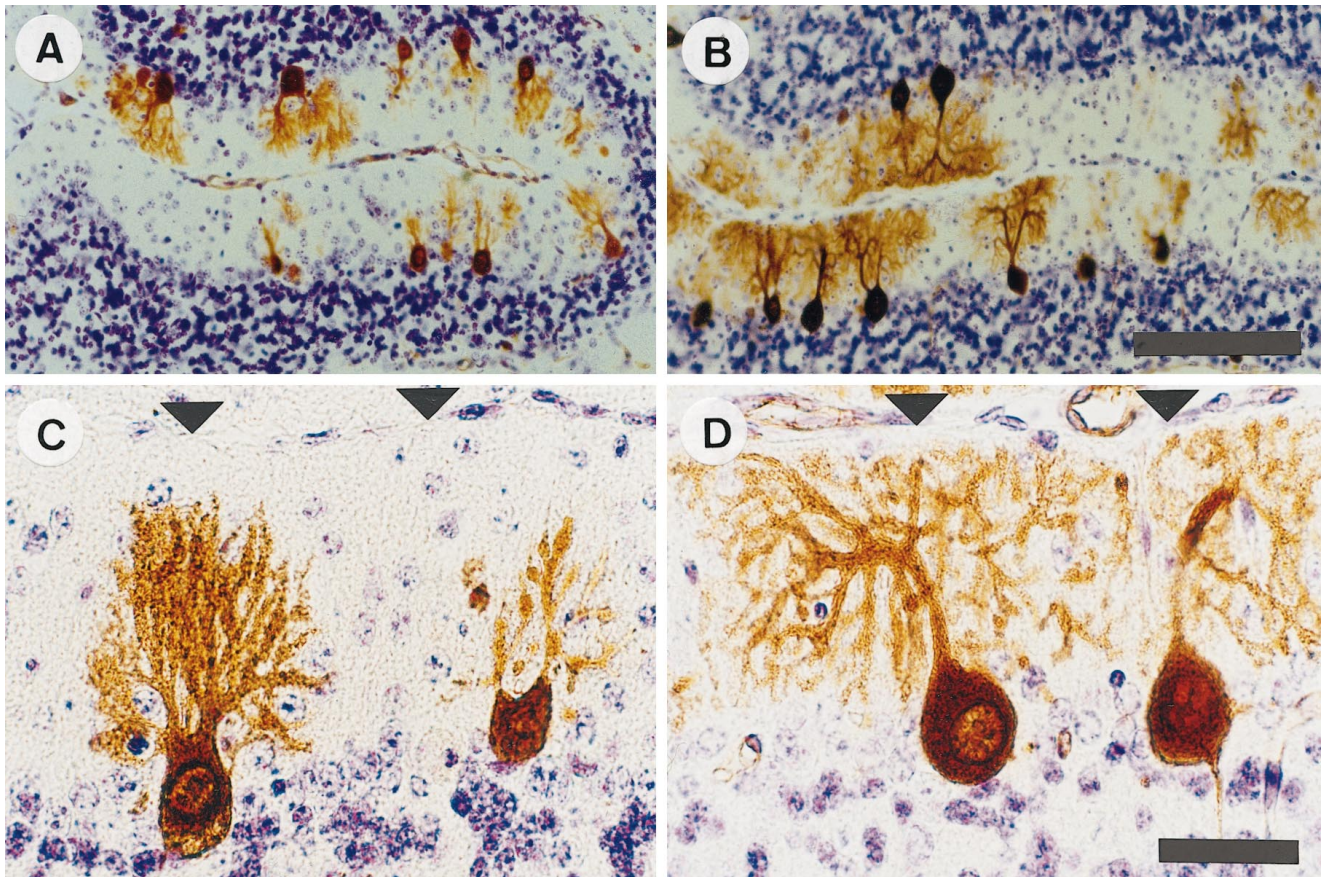
Figure 2. Increased Purkinje cell dendritic growth and branching in Lurcher (+/*Lc*) mice after the destruction of granule cells with x rays. Midsagittal cerebellar sections of P20 mice processed for anti-Calbindin immunocytochemistry and cresyl violet–thionin staining. *A, C*, Nonirradiated +/*Lc* mouse. *B, D*, X-irradiated +/*Lc* mouse. The micrographs are taken from the preculminate fissure in the anterior cerebellum (lobules 3 and 4). *Arrowheads* indicate the pial surface. Scale bars: *A, B*, 100 μm; *C, D*, 25 μm.
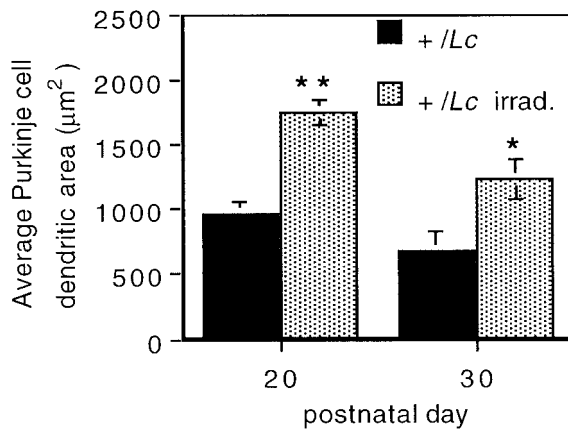
are the inverse: Purkinje cell dendritic trees were considerably smaller and less complex than those of normal controls (data not shown) (for previous demonstration, see Altman and Bayer, 1997). The dendrites of Purkinje cells in sections from both x-irradiated and nonirradiated +/*Lc* mice were invested with spines.

To compare quantitatively the dendritic morphology of Purkinje cells in sections of x-irradiated and nonirradiated +/*Lc* mice, we measured the area enclosed by the dendritic tree using image analysis. The analysis was performed on sections from P20 and P30 mice ($n = 3$ for each group) and revealed a significantly larger area covered by +/*Lc* Purkinje cell dendrites in the x-irradiated mice (Fig. 3). This increased dendritic growth after x irradiation is greatest at P20 (1755 $\pm$ 100 μm^2 vs 969 $\pm$ 100 μm^2 in the nonirradiated +/*Lc*; $p < 0.01$), but the difference remains significant for the small population of Purkinje cells that persist at P30 (1240 $\pm$ 155 μm^2 vs 683 $\pm$ 119 μm^2 in the nonirradiated +/*Lc*; $p < 0.05$). The measurement of the height of CaBP-immunolabeled Purkinje cells from the base of the soma to the tip of the dendritic tree indicates that the vast majority of increased dendritic growth is in the lateral plane: the average height of Purkinje cells in sections of x-irradiated and nonirradiated +/*Lc* mice are comparable at P15, P20, and P25 (data not shown). At P30, the average height of Purkinje cells in sections of x-irradiated +/*Lc* mice is slightly greater (53.8 $\pm$ 2.9 μm vs 41.5 $\pm$ 3.3 μm in the nonirradiated +/*Lc*; $p < 0.05$). These results

indicate that the destruction of granule cells in young +/*Lc* mice by x irradiation results in increased Purkinje cell dendritic growth and branching that is primarily in the lateral plane. The greater increase of dendritic growth in the lateral direction is likely to be a consequence of the shallow depth of the ML in x-irradiated +/*Lc* mice, because the dendritic trees of well developed Purkinje cells invariably extended to the pial surface. The increased dendritic growth in x-irradiated +/*Lc* mice suggest that the normal trophic effects of granule cell interaction on Purkinje cell development are absent in the mutant.

Partial destruction of granule cells by x rays does not alter the rate of +/*Lc* Purkinje cell death

Purkinje cell death in +/*Lc* mice begins in the second postnatal week and is rapid and total: by P26, 90% of the Purkinje cells have died (Caddy and Biscoe, 1979). We examined the effects of decreased granule interaction on +/*Lc* Purkinje cell death by comparing Purkinje cell numbers in x-irradiated and nonirradiated mice at P15, P20, P25, and P30 ($n = 3–5$ animals per group), using the same midsagittal cerebellar sections processed for anti-CaBP immunocytochemistry for the measures of dendritic development. The number of Purkinje cells per midsagittal cerebellar section was counted as a sample of the size of the Purkinje cell population (Fig. 4). Identical counts were performed on midsagittal sections from P15 +/+ mice ($n = 3$) and reveal an average of 643 $\pm$ 13 Purkinje cells per section. At P15, gaps are already

Figure 3. Increased Purkinje cell dendritic area in Lurcher (+/*Lc*) mice after the destruction of granule cells with x rays. The area encompassed by the Purkinje cell dendritic tree was measured from midsagittal cerebellar sections of P20 mice processed for anti-Calbindin immunocytochemistry. Ten to 20 Purkinje cells were analyzed per animal. Error bars indicate SEM ($n = 3$). *Asterisks* denote statistically significant differences: *$p < 0.05$; **$p < 0.01$ (unpaired two-tailed Student's *t* test).

observed in the PCL in sections of +/*Lc* cerebella, and the number of Purkinje cells per section is 70% of the +/+ value. A similar immunostaining pattern is observed in the sections of P15 x-irradiated +/*Lc* mice (indicating the existence of Purkinje cell death) and this is confirmed by the cell counts that indicate that the number of Purkinje cells is only 60% of the +/+ value. The cell counts of P20, P25, and P30 mice reveal a dramatic decline in +/*Lc* Purkinje cell numbers in the sections of both x-irradiated and nonirradiated +/*Lc* mice. At P30, the loss of Purkinje cells is near total, and the number of cells is only 5% of the P15 +/+ value in the sections from x-irradiated and nonirradiated +/*Lc* mice. These results demonstrate that the partial destruction of granule cells by x irradiation does not affect the rate of +/*Lc* Purkinje cell death. The unaltered rate of cell death in the x-irradiated mutants indicates that there are two separable components to Purkinje cell abnormalities in +/*Lc* mice: a retardation/blockade of dendritic development that is mediated by interactions with granule cells and the death of the cell.

Decreased ultrastructural abnormalities in +/*Lc* mice following the destruction of granule cells with x rays

The poor development of Purkinje cells in +/*Lc* mice is accompanied by a well documented pattern of abnormal ultrastructural features. When examined in the electron microscope, the nuclear chromatin of +/*Lc* Purkinje cells is clumped, the nuclear membrane is irregular, and the cytoplasmic organelles are disorganized: the rough endoplasmic reticulum fails to form Nissl bodies, the Golgi apparatus is scattered, and the mitochondria appear swollen with spherical profiles (Caddy and Biscoe, 1979; Dumesnil-Bousez and Sotelo, 1992). We tested the possibility that the increased Purkinje cell dendritic development observed in x-irradiated +/*Lc* mice is accompanied by a reduction in the ultrastructural abnormalities associated with the effects of the mutation. We examined cerebellar sections from P20 x-irradiated and nonirradiated +/*Lc* mice in the electron microscope (Fig. 5). Ultrastructural abnormalities characteristic of the mutation could be observed in Purkinje cells in sections from both x-irradiated and nonirradiated mice (as could gaps in the PCL and electron-dense and vacuolated Purkinje cells, confirming the presence of large-scale Purkinje cell death). However, Purkinje cell bodies
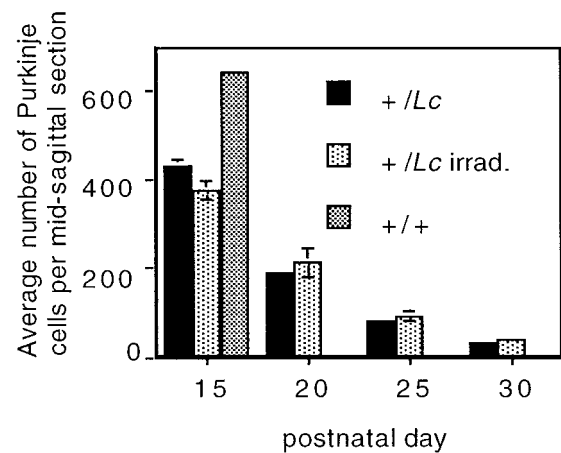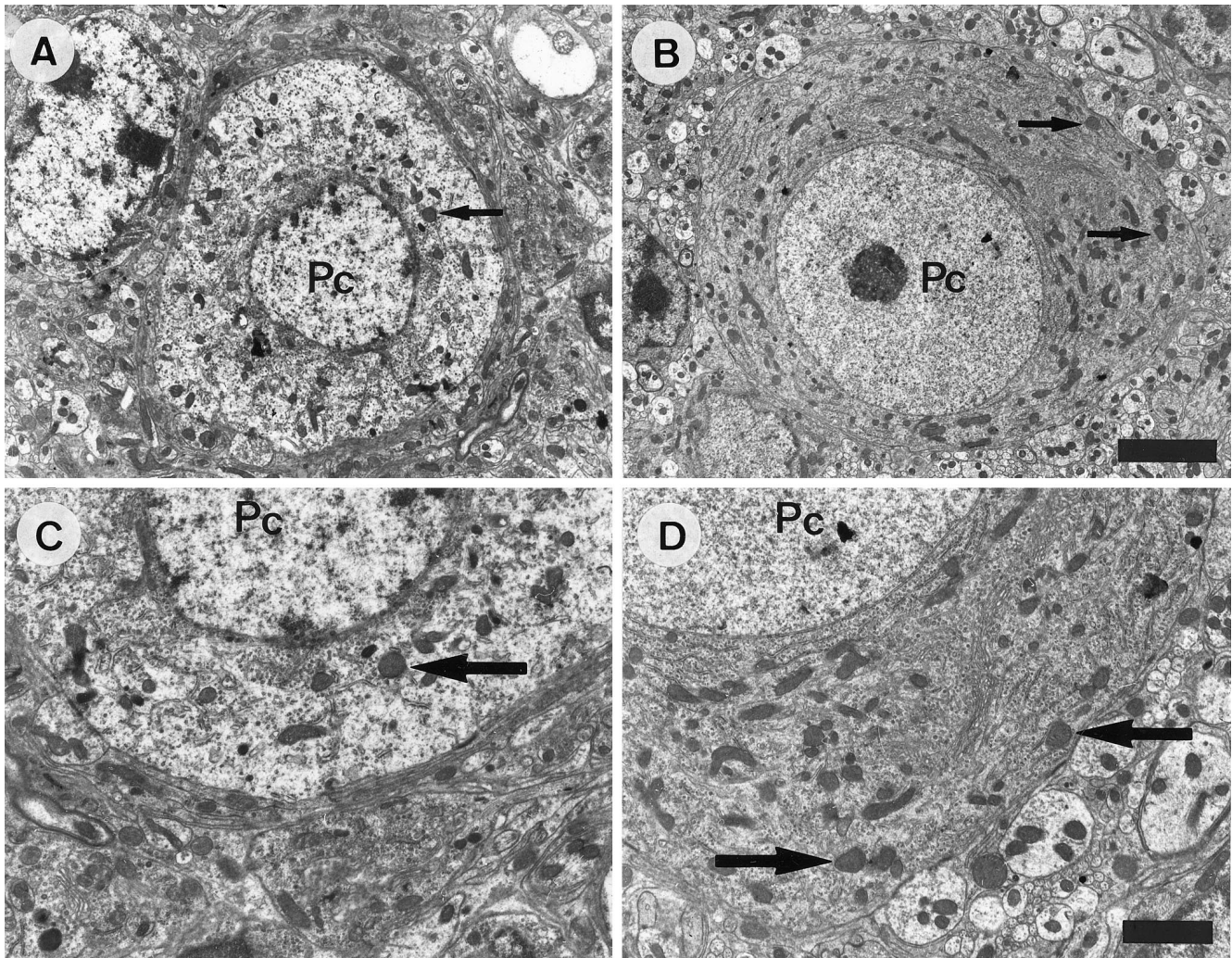

Figure 4. The destruction of granule cells by x irradiation does not affect the rate of Lurcher (+/*Lc*) Purkinje cell death. The cell counts were performed on midsagittal cerebellar sections processed for anti-Calbindin immunocytochemistry to aid the identification of Purkinje cells in the disrupted cerebellar cortex of x-irradiated mice. The data are presented as the number of Purkinje cells per section. Error bars indicate SEM ($n = 3–5$).

containing spherical, electron-lucent nuclei (with a prominent nucleolus) encircled by Nissl bodies, Golgi apparatus, and mitochondria could be observed in sections from x-irradiated +/*Lc* mice. These ultrastructural features are more reminiscent of +/+ Purkinje cells and were never observed in sections from the nonirradiated +/*Lc* mice. Although the organization of the cytoplasmic organelles in these Purkinje cells in x-irradiated mice appeared normal, swollen mitochondrial profiles were present, indicating some abnormality. The appearance of more healthy looking Purkinje cells in the sections of x-irradiated compared with nonirradiated +/*Lc* mice indicates that granule cell destruction results in a delay in the disruption of the ultrastructure of the cell. The data suggest that interactions with granule cells are a contributory factor in the disruption of the cytoplasmic structure, as well as the poor dendritic development, of +/*Lc* Purkinje cells.

The increased conductance of +/*Lc* Purkinje cells is not affected by the destruction of granule cells with x rays

The large inward current produced by the mutation of the GluRδ2 gene in +/*Lc* mice results in a chronic depolarization of the resting membrane potential that is independent of any known ligand (Zuo et al., 1997) and is therefore not expected to be affected by the destruction of granule cells with x rays. We investigated this hypothesis by recording the electrophysiological properties of Purkinje cells in slices of the cerebellar vermis of P15–P20 x-irradiated and nonirradiated +/*Lc* and +/+ mice (Fig. 6). Although +/*Lc* Purkinje cells are already compromised by the mutation at P15–P20, the cells could be held long enough in the whole-cell recording mode to obtain sufficient responses (≥ 20 min). In agreement with the results of Zuo et al. (1997), we found that the resting membrane potential of Purkinje cells in nonirradiated +/*Lc* slices was depolarized (-27.8 ± 1.0 mV; $n = 6$) in comparison to +/+ cells (-50.6 ± 2.3 mV; $n = 8$), and the size of the current required to hold the cell at -70 mV was considerably larger (-2250 ± 254 pA in +/*Lc* Purkinje cells compared with -220 ± 20 pA in +/+ cells). Recordings from x-irradiated mice produced similar results. The resting membrane potential of Purkinje cells in x-irradiated +/*Lc* mice was depolarized

Figure 5. Decreased ultrastructural abnormalities in +/*Lc* Purkinje cells after the destruction of granule cells with x rays. The micrographs are taken from sagittal sections of the cerebellar vermis of P20 mice. Low- and high-power micrographs of a Purkinje cell in nonirradiated (*A, C*) and x-irradiated (*B, D*) Lurcher (+/*Lc*) mice. The Purkinje cell (*Pc*) in the micrographs taken from the nonirradiated +/*Lc* mouse displays abnormalities characteristic of the mutation: the nuclear chromatin is clumped, the nuclear membrane is irregular, and the cytoplasmic organelles are disorganized: the rough endoplasmic reticulum is not arranged into Nissl bodies, and the mitochondria are distended with spherical profiles. In contrast, the Purkinje cell (*Pc*) in the micrograph taken from the x-irradiated +/*Lc* mouse has a relatively normal appearance: the soma contains a spherical, electron-lucent nucleus (with a prominent nucleolus) that is encircled by normal-appearing mitochondria and Nissl bodies. The *arrows* point to swollen mitochondrial profiles. Scale bars: *A, B,* 4 μm; *C, D,* 2 μm.

(-31.0 ± 1.3 mV; $n = 11$) when compared with +/+ littermates exposed to the same x-ray dose (-62.3 ± 2.4 mV; $n = 10$), and the magnitude of the current required to hold the cell at -70 mV was again much larger (-2078 ± 167 pA in +/*Lc* Purkinje cells and -262 ± 52 pA in +/+ cells).

To establish that the leak currents recorded in +/*Lc* cells were not a consequence of nonspecific poor recording conditions, we repeated the experiment of Zuo et al. (1997) and substituted NMDG, a large organic cation, for the majority of Na$^+$ in the external saline. In the presence of NMDG, the magnitude of the current required to hold +/*Lc* Purkinje cells at -70 mV was dramatically decreased in slices from x-irradiated (-2078 ± 167 to -338 ± 82 pA) and nonirradiated (-2250 ± 254 to -140 ± 40 pA) mice. The substitution of Na$^+$ with NMDG also resulted in a slight reduction of the size of the holding current required for +/+ Purkinje cells in slices from x-irradiated (-262 ± 52 to -123 ± 30 pA) and nonirradiated (-220 ± 20 to -96 ± 19 pA) mice, but the decrease was of a considerably

smaller magnitude. Taken together, the data demonstrate that the increased conductance of +/*Lc* Purkinje cells is not affected by the destruction of granule cells with x rays. Thus, the increased dendritic development and decreased ultrastructural abnormalities of Purkinje cells in x-irradiated +/*Lc* mice are not a consequence of an alteration in the activity of the mutated GluRδ2^{Lc} channel. Rather, interactions with the granule cells that normally promote Purkinje cell differentiation act to restrict the development of the cell in +/*Lc* mice.

DISCUSSION

There is considerable evidence from studies conducted on cell culture and animal models that interactions with granule cells are required for the normal dendritic differentiation of Purkinje cells (Sotelo, 1975; Mariani et al., 1977; Baptista et al., 1994; Altman and Bayer, 1997; Mason and Morrison, 1998). In this study, we have demonstrated that the partial destruction of the granule cell population in young +/*Lc* mice results in increased Purkinje cell
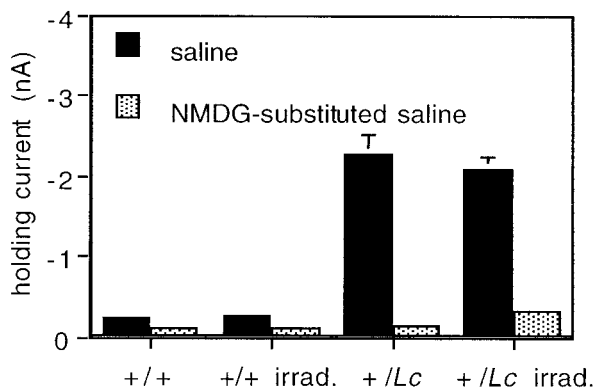
Figure 6. The increased conductance of +/*Lc* Purkinje cells is not affected by the destruction of granule cells with x rays. The size of the current required to hold the Purkinje cell at −70 mV was measured in sagittal cerebellar slices of P15–P20 mice. The large magnitude of the holding currents of Purkinje cells in slices from nonirradiated and x-irradiated +/*Lc* mice was decreased by the substitution of the large organic cation NMDG for the majority of the sodium in the external saline solution. Error bars indicate SEM (*n* = 6–11).

dendritic growth and branching. The examination of +/*Lc* Purkinje cells in the electron microscope revealed that the increase in dendritic growth was accompanied by a delay in the disruption of the ultrastructure of the cell associated with the mutation. In contrast, the early destruction of granule cells with x rays was shown to have no effect on the rate of Purkinje cell death in +/*Lc* mice.

Negative effect of granule cell interaction on +/*Lc* Purkinje cell dendritic growth

The negative effect of granule cells on the development of +/*Lc* Purkinje cells suggests that the effects of granule cell interaction are dependent on the state of the target cell. The regulation of target cell development by afferents has been demonstrated to be via both activity-dependent and nonactivity-dependent mechanisms (Kossel et al., 1997). Of the many possible regulatory mechanisms, neurotrophic signaling appears to be widely implicated in the control of dendritic development (McAllister et al., 1997). In the cerebellum, the neurotrophins BDNF and NT-3 have been shown to regulate Purkinje cell dendritic development (Neveu and Arenas, 1996; Schwartz et al., 1997). Recent experiments performed on purified cell cocultures have demonstrated that Purkinje cell responses to neurotrophins are highly modulated by granule cell activity, suggesting that the survival and differentiation of the cell are context-dependent (Morrison and Mason, 1998). The compromised state of the Purkinje cells of +/*Lc* mice is evidently sufficient to negate the normal trophic effects of granule cell interaction *in vivo*.

A number of studies have suggested that fluctuations in the levels of intracellular free calcium are responsible for the activity-dependent regulation of dendritic development (Schilling et al., 1991; Kossel et al., 1997; Metzger et al., 1998). The cessation of growth and initiation of branching of Purkinje cell dendrites in culture coincides with the onset of electrical activity and can be inhibited by the blockade of voltage-dependent sodium channels with tetrodotoxin (TTX) (Schilling et al., 1991). At the time that branching begins in culture, the intracellular calcium levels of Purkinje cells become sensitive to TTX, suggesting that calcium might mediate the effect of activity on dendritic growth. In the

cerebellar cortex, the excitatory synaptic activation of the Purkinje cells is provided by olivocerebellar climbing fiber and granule cell parallel fiber afferents. The selective lesion of either of these afferents *in vivo* has indicated that parallel fibers exert the far stronger influence on Purkinje cell dendritic development (Sotelo and Arsenio-Nunes, 1976; Altman and Bayer, 1997). Taken together, these studies suggest that calcium influx after activation of glutamate receptors at parallel fiber synapses could regulate the development of Purkinje cell dendrites. In +/*Lc* mice, the depolarized resting membrane potential of Purkinje cells (approximately −30 mV) is in the range of activation of voltage-dependent calcium channels (Mouginot et al., 1997). The dendrites of +/*Lc* Purkinje cells are therefore likely to have elevated basal levels of intracellular free calcium that are further augmented by synaptic activity. We speculate that synaptic depolarization of +/*Lc* Purkinje cells raises the elevated basal levels of intracellular free calcium to supraoptimal concentrations that act to restrict rather than promote dendritic growth.

Granule cell destruction does not affect the rate of +/*Lc* Purkinje cell death

It has been suggested that the Purkinje cells in +/*Lc* mice die an excitotoxic cell death as a result of the large, constitutive inward current produced by the mutation of the GluRδ2 gene (Zuo et al., 1997). The data presented here are consistent with this hypothesis. We have shown that the partial destruction of granule cells does not alter the rate of +/*Lc* Purkinje cell death or the conductance of the GluRδ2^{Lc} channel.

The mechanisms by which Purkinje cell death is triggered in +/*Lc* mice have not been resolved. Lurcher Purkinje cell death begins in the second postnatal week, long after the GluRδ2 protein is first detected in +/+ mice: GluRδ2 immunoreactivity is expressed in Purkinje cells as early as embryonic day 15 (Takayama et al., 1996). Thus, there appears to be a mismatch between the timing of +/*Lc* Purkinje cell death and the reported expression of the normal GluRδ2 protein in +/+ mice. Our data suggest that +/*Lc* Purkinje cell death may be independent of granule cell interaction and is likely to be a direct consequence of GluRδ2^{Lc} conductance. The question therefore arises as to whether the mutated GluRδ2^{Lc} protein acts as a channel before Purkinje cell death in +/*Lc* mice. For instance, does the GluRδ2^{Lc} protein only act as a channel when localized to the Purkinje cell dendritic spines (during normal postnatal development, GluRδ2 becomes localized to the dendritic spines of Purkinje cells; see Takayama et al., 1996)? If this is the case, the putative mechanisms restricting GluRδ2^{Lc} activity in young +/*Lc* Purkinje cells are not present in the simpler oocyte system, because the expression of GluRδ2^{Lc} cRNA in oocytes produces a conductance similar to that observed in +/*Lc* Purkinje cells (Zuo et al., 1997). Alternatively, the timing of +/*Lc* Purkinje cell death may be determined by other factors related to the maturational state of the cell (Norman et al., 1995), such as the expression of downstream effector proteins or the assembly of voltage-dependent calcium channels. The timing of Purkinje cell death varies from cell to cell in +/*Lc* mice, and it is possible that cell-specific differences in the timing of expression or maturation of any of these candidate cell death-initiating factors could account for this variation.

Certain features of Purkinje cells in +/*Lc* mice have led to the speculation that the cell dies an apoptotic death (Norman et al., 1995). In agreement with this hypothesis, others in our laboratory have found that caspase-3, an aspartate-specific cysteine protease

that is an essential effector of apoptosis (Nicholson and Thornberry, 1997), is expressed in dying +/*Lc* Purkinje cells (F. Selimi and J. Mariani, unpublished observations). Recently, a number of studies have indicated a role for mitochondria in the initiation of apoptosis (for review, see Reed, 1997). In particular, mitochondrial swelling similar to that observed in +/*Lc* Purkinje cells is induced by a wide variety of apoptotic stimuli (Vander Heiden et al., 1997). In these examples of apoptosis, mitochondrial swelling resulted in the release of cytochrome *c* from the intermembrane space to the cytosol, which is thought to subsequently trigger the apoptotic process (Vander Heiden et al., 1997). The depolarization of the +/*Lc* Purkinje cell by GluRδ2^{Lc} conductance would be expected to result in less favorable conditions for the maintenance of the mitochondrial membrane potential. An impairment of mitochondrial function will deplete the production of ATP by the cell as well as have serious consequences for the homeostasis of the organelle itself. Functioning mitochondria maintain a higher internal osmolarity than the cytosol. Thus, the swollen mitochondria observed in +/*Lc* Purkinje cells may indicate osmotic swelling as a result of impaired function in response to the depolarizing conditions in the cell. In this manner, the GluRδ2^{Lc} conductance could disrupt mitochondrial function, leading to the swelling of the organelle, the release of cytochrome *c* into the cytosol, and the initiation of apoptosis. The detection of swollen mitochondrial profiles in the differently developed but equally vulnerable Purkinje cells of both x-irradiated and nonirradiated +/*Lc* mice in this study is consistent with this idea.

Two components to Purkinje cell abnormalities in +/*Lc* mice

In conclusion, we have demonstrated two components to Purkinje cell abnormalities in +/*Lc* mice: a retardation/blockade of dendritic development that is mediated by interactions with granule cells and the subsequent death of the cell. We speculate that the restricted dendritic development of +/*Lc* Purkinje cells could be a consequence of excess levels of intracellular free calcium in the dendrites in response to parallel fiber activity. The negative effect of granule cell interaction in +/*Lc* mice supports the idea that Purkinje cell responses are context-dependent. The rate of Lurcher Purkinje cell death, on the other hand, was not affected by the reduction in granule cell number and may be triggered by the impairment of mitochondrial function in response to the depolarizing conditions created by the GluRδ2^{Lc} conductance. We hope to investigate these hypotheses in the future using vital fluorescent indicators of intracellular free calcium concentration and mitochondrial membrane potential.

REFERENCES

Altman J, Bayer SA (1997) Development of the cerebellar system in relation to its evolution, structure and functions. Boca Raton: CRC.

Baird DE, Hatten ME, Mason CA (1992) Cerebellar target neurons provide a stop signal for afferent neurite extension *in vitro*. J Neurosci 12:619–634.

Baird DE, Trenkner E, Mason CA (1996) Arrest of afferent axon extension by target neurons *in vitro* is regulated by the NMDA receptor. J Neurosci 16:2642–2648.

Baptista CA, Hatten ME, Blazeski R, Mason CA (1994) Cell-cell interactions influence survival and differentiation of purified Purkinje cells *in vitro*. Neuron 12:243–260.

Caddy KWT, Biscoe T (1979) Structural and quantitative studies on the normal C3H and Lurcher mutant mouse. Philos Trans R Soc Lond B Biol Sci 287:167–201.

Crepel F, Delhaye-Bouchaud N, Legrand J (1976) Electrophysiological

analysis of the circuitry of the cortico-nuclear relationships in the agranular cerebellum of irradiated rats. Arch Ital Biol 114:49–74.

Davis GW, Schuster CM, Goodman CS (1997) Genetic analysis of the mechanisms controlling target selection: target-derived Fasciclin II regulates the pattern of synapse formation. Neuron 19:561–573.

Dumesnil-Bousez N, Sotelo C (1992) Early development of the Lurcher cerebellum: Purkinje cell alterations and impairment of synaptogenesis. J Neurocytol 21:506–529.

Feddersen RM, Ehlenfeldt R, Yunis WS, Clark HB, Orr HT (1992) Disrupted cerebellar cortical development and progressive degeneration of Purkinje cells in SV40 T antigen transgenic mice. Neuron 9:955–966.

Hatten ME, Alder J, Zimmerman K, Heintz N (1997) Genes involved in cerebellar cell specification and differentiation. Curr Opin Neurobiol 7:40–47.

Herrup K, Sunter K (1986) Cell lineage dependent and independent control of Purkinje cell number in the mammalian CNS: further quantitative studies of lurcher chimeric mice. Dev Biol 117:417–427.

Kossel AH, Williams CV, Schweizer M, Kater SB (1997) Afferent innervation influences the development of dendritic branches and spines via both activity-dependent and non-activity-dependent mechanisms. J Neurosci 18:1735–1742.

Kurihara H, Hashimoto K, Kano M, Takayama C, Sakimura K, Mishina M, Inoue Y, Watanabe M (1997) Impaired parallel fibre-Purkinje cell synapse stabilization during cerebellar development of mutant mice lacking the glutamate receptor δ2 subunit. J Neurosci 17:9613–9623.

Landsend AS, Amiry-Moghaddam M, Matsubara A, Bergersen L, Usami S, Wenthold RJ, Ottersen OP (1997) Differential localization of δ glutamate receptors in the rat cerebellum: coexpression with AMPA receptors in parallel fibre-spine synapses and absence from climbing fibre-spine synapses. J Neurosci 17:834–842.

Legrand C, Thomasset M, Parkes CO, Clavel M, Rabie A (1983) Calcium-binding protein in the developing rat cerebellum. An immunocytochemical study. Cell Tissue Res 233:389–402.

Llano I, Marty A, Armstrong CM, Konnerth A (1991) Synaptic and agonist induced excitatory currents of Purkinje cells in rat cerebellar slices. J Physiol (Lond) 434:183–213.

Mariani J, Crepel F, Mikoshiba K, Changeux JP, Sotelo C (1977) Anatomical, physiological and biochemical studies of the cerebellum from reeler mutant mouse. Philos Trans R Soc Lond B Biol Sci 281:1–28.

McAllister AK, Katz LC, Lo DC (1997) Opposing roles for endogenous BDNF and NT-3 in regulating cortical dendritic growth. Neuron 18:767–778.

Metzger F, Wiese S, Sendtner M (1998) Effect of glutamate on dendritic growth in embryonic rat motoneurons. J Neurosci 1:1735–1742.

Morrison ME, Mason CA (1998) Granule neuron regulation of Purkinje cell development: striking a balance between neurotrophin and glutamate signalling. J Neurosci 18:3563–3573.

Mouginot D, Bossu JL, Gahwiler BH (1997) Low-threshold Ca2+ currents in dendritic recordings from Purkinje cells in rat cerebellar slice cultures. J Neurosci 17:160–170.

Neveu I, Arenas B (1996) Neurotrophins promote the survival and development of neurons in the cerebellum of hypothyroid rats *in vivo*. J Cell Biol 133:631–646.

Nicholson DW, Thornberry NA (1997) Caspases: killer proteases. Trends Biochem Sci 22:299–306.

Norman DJ, Feng L, Cheng SS, Gubbay J, Chan E, Heintz N (1995) The lurcher gene induces apoptotic death in cerebellar Purkinje cells. Development 121:1183–1193.

Ozaki M, Sasner M, Yano R, Lu HS, Buonanno A (1997) Neuregulin-β induces expression of an NMDA-receptor subunit. Nature 390:691–694.

Porter BE, Weis J, Sanes JR (1995) A motorneuron-selective stop signal in the synaptic protein S-laminin. Neuron 14:549–559.

Reed JC (1997) Cytochrome c: can't live with it - can't live without it. Cell 91:559–562.

Schilling K, Dickinson MH, Connor JA, Morgan JI (1991) Electrical activity in cerebellar cultures determines Purkinje cell dendritic growth patterns. Neuron 7:891–902.

Schwartz PM, Borghesani PR, Levy RL, Pomeroy SL, Segal RA (1997) Abnormal cerebellar development and foliation in BDNF−/− mice reveals a role for neurotrophins in CNS patterning. Neuron 19:269–281.

Sotelo C (1975) Anatomical, physiological and biochemical studies of the cerebellum from mutant mice. II. Morphological study of cerebellar cortical neurons and circuits in the Weaver mouse. Brain Res 94:19–44.

Sotelo C, Arsenio-Nunes ML (1976) Development of Purkinje cells in absence of climbing fibers. Brain Res 111:389–395.

Sotelo C, Changeux JP (1974) Transynaptic degeneration "en cascade" in the cerebellar cortex of staggerer mutant mice. Dev Brain Res 67:519–526.

Takayama C, Nakagawa S, Watanabe M, Mishina M, Inoue Y (1996) Developmental changes in expression and distribution of the glutamate receptor channel δ2 subunit according to the Purkinje cell maturation. Dev Brain Res 92:147–155.

Tessier-Lavigne M, Goodman CS (1996) The molecular biology of axon guidance. Science 274:1123–1133.

Vander Heiden MG, Chel NS, Williamson EK, Schumacker PT, Thompson CB (1997) Bcl-x$_L$ regulates the membrane potential and volume homeostasis of mitochondria. Cell 91:627–637.

Wood KA, Youle RJ (1995) The role of free radicals and p53 in neuron apoptosis *in vivo*. J Neurosci 15:5851–5857.

Yoon CH (1976) Pleiotropic effect of the staggerer gene. Brain Res 109:206–215.

Zuo J, De Jager PL, Takahashi KA, Jiang W, Linden DJ, Heintz N (1997) Neurodegeneration in Lurcher mice caused by mutation in δ2 glutamate receptor gene. Nature 388:769–773.